Angle-resolved photoemission spectroscopy

Mengyu Yao[#], Gerhard Fecher[##], Claudia Felser

Angle-resolved photoemission spectroscopy (ARPES) is one of the foremost experimental techniques applied in cutting-edge condensed matter physics research, enabling the electronic structure of diverse systems to be studied directly. The ARPES group of the solid-state chemistry department are interested in solving electronic-structure-related problems. Here, we apply ARPES to analyze the structures of topological materials, such as topological superconductors, chiral materials, and iron-based superconductors. Moreover, we reveal the electronic structures of thermoelectric materials.

In the past decade, the realization of topological phases in solids has emerged as an important subject in experimental condensed matter physics. Topological materials are characterized by low-energy excitations (quasiparticles) near the band-crossing points, with examples including Dirac semimetals and type-I and type-II Weyl semimetals. Originally predicted by high-energy physics, condensed matter physicists classify these quasiparticles according to their electronic structure [1-3]. Elucidating the electronic structure of materials is vital for research in many fields, for example thermoelectric devices and catalysis [4].

Angle-resolved photoemission spectroscopy (ARPES) is an experimental technique based on the photoelectric effect [5]. It is the most powerful tool for probing the electronic structure of solids. In recent decades, remarkable advances have been made in the application of ARPES, including the development of soft X-ray ARPES and spin-resolved ARPES. The energy of incident photons is an important parameter in ARPES. Owing to the progress made in synchrotron technology, the energy range of photons for experimental research has expanded considerably. At present, lamp-based vacuum ultraviolet (VUV) light, lasers, and synchrotron-based X-rays are the most common photon sources for ARPES.

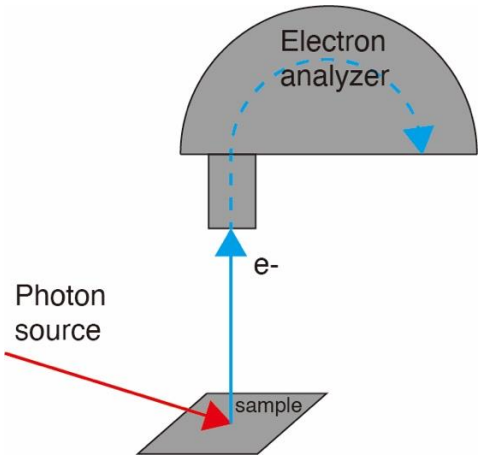

Fig. 1. Principle of angle-resolved photoemission spectroscopy.

The ARPES group of the solid-state chemistry department uses ARPES and related techniques to investigate the electronic structure of various materials. Our lab-based ARPES system is integrated with a helium-charged VUV lamp, a twin-anodes X-ray source and a Scienta-Omicron DA30 detector. This system allows us to perform preliminary research on newly synthesized samples. In addition, we collaborate with many synchrotron-based ARPES labs in Europe and China. To date, we have applied ARPES to analyze topological superconductors, thermoelectric materials, chiral materials, and iron-based superconductors. This article summarizes some of the most important contributions of our research group.

Six-fold degenerate fermions in superconductors

Both Dirac and Weyl semimetals have been shown to exhibit quasiparticle excitations that mimic the wavefunctions of exotic fermions predicted by high-energy physics. However, condensed matter systems can realize novel fermions that have no counterpart in high-energy physics. The six-fold degenerate fermion, otherwise known as the sextuple point, is one such fermion. We showed that sextuple points with a vanishing Chern number exist, implying the absence of surface Fermi arcs. In this case, we revealed the existence of sextuple points in superconducting $PdSb_2$.

A sextuple point originates where a twofold and a nondegenerate band cross. Therefore, it has a bulk band structure that depends on its position in momentum space. In $PdSb_2$, sextuple points are predicted to occur at the corners (R points) of the three-dimensional Brillouin zone (BZ), as shown in Fig. 2(a). To explore these sextuple points, we performed high-resolution ARPES measurements. For soft X-rays, ARPES operates with a photon energy above ~ 200 eV. Within the soft x-ray energy region, the photoemission from the bulk states dominates. We use this feature to perform k_z-dependent measurements, which inform the selection of photon energies corresponding the R points. The Fermi surface (FS) intensity plots are shown in Fig. 2 (b,c). Furthermore, high-resolution

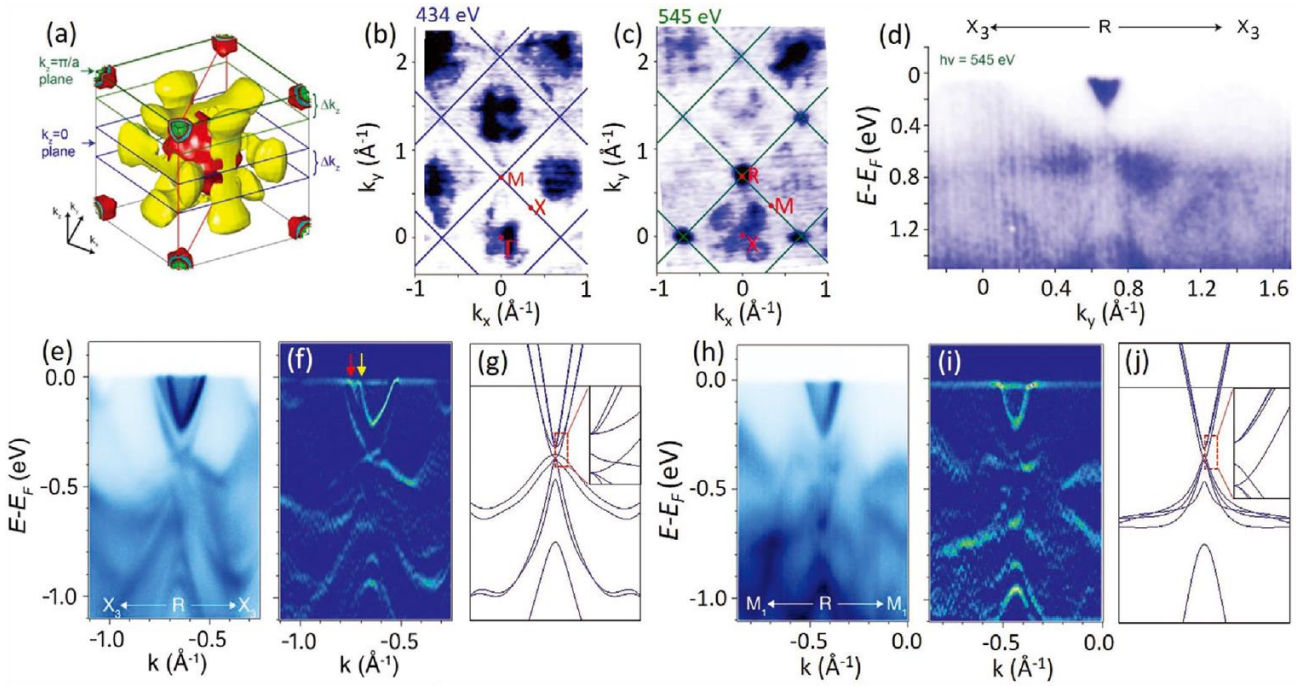

Fig. 2: Electronic structure of $PdSb_2$. (a) Calculated 3D Fermi surface. (b) Measured Fermi surface in the $k_z = 0$ plane. (c) Measured Fermi surface in the $k_z = \pi/a$ plane. (d) Measured band dispersion along the X_3–R–X_3 direction. (e) Measured band dispersion along the X_3–R–X_3 direction. (f) Curvature intensity plot corresponding to (e). (g) Calculated band structure along the X_3−R−X_3 direction. (h–j) ARPES intensity plot, corresponding curvature intensity plot, and calculated band structure along the M_1−R−M_1 direction.

ARPES spectra were obtained to resolve the detailed band structures, which were compared with theoretical predictions. From the ARPES intensity plots (Fig. 2 (e,h)), the crossing site appears at ~ 0.25 eV below the Fermi energy. The ARPES spectra were consistent with theoretical predictions. Thus, we demonstrated the existence of a sub-Fermi energy sextuple point in a superconducting pyrite [6].

Electronic structure of 3D half-Heusler thermo-electric materials

Thermoelectric materials are a broad category of materials attracting attention not only from the scientific community but also manufacturers. Thermoelectric technology, which converts heat into electricity, or vice versa, exhibits promise for applications in a variety of fields. It is well established that narrow-bandgap semiconductors make for the best thermoelectric materials because of their characteristic electronic structure. The bandgap, E_g, which is one of the key parameters derived from the electronic structure, is central to the excellent thermoelectric performance of narrow-bandgap semiconductors. Therefore, the accurate determination of the intrinsic electronic structure of thermoelectric materials is a prerequisite for utilizing electronic-band engineering to improve their thermoelectric performance.

Half-Heusler alloys are magnetic intermetallic compounds that comprise an exciting class of thermoelectric materials. The first half-Heusler thermoelectric system that was discovered, *M*NiSn, serves as a ripe platform for exploring the intrinsic origin of high power factors (PF). Recently, large density of states near the Fermi energy, low deformation potential, and high band degeneracy have been recognized as important factors that contribute to a high PF. However, several problems related to the electronic structure of *M*NiSn remain unresolved, such as "the real E_g of *M*NiSn."

This issue can be resolved by performing high-resolution ARPES studies on ZrNiSn, which enables direct observation of the intrinsic electronic structure. By using photon energies ranging from 60 to 160 eV, we captured the electronic structure of ZrNiSn within an entire 3D BZ. The conduction band at the X point was clearly resolved, agreeing with the calculated electronic structure. To analyze the intrinsic electronic structure in greater depth, the 2D ARPES intensity plot within the $k_z = 0$ plane was acquired, allowing us to observe the band structure between the Γ point (the valence band maximum) and the X point (the conduction band minimum) simultaneously. As a result, the band gap of 0.66 ± 0.1 eV measured directly from ARPES spectra was approximately two to three

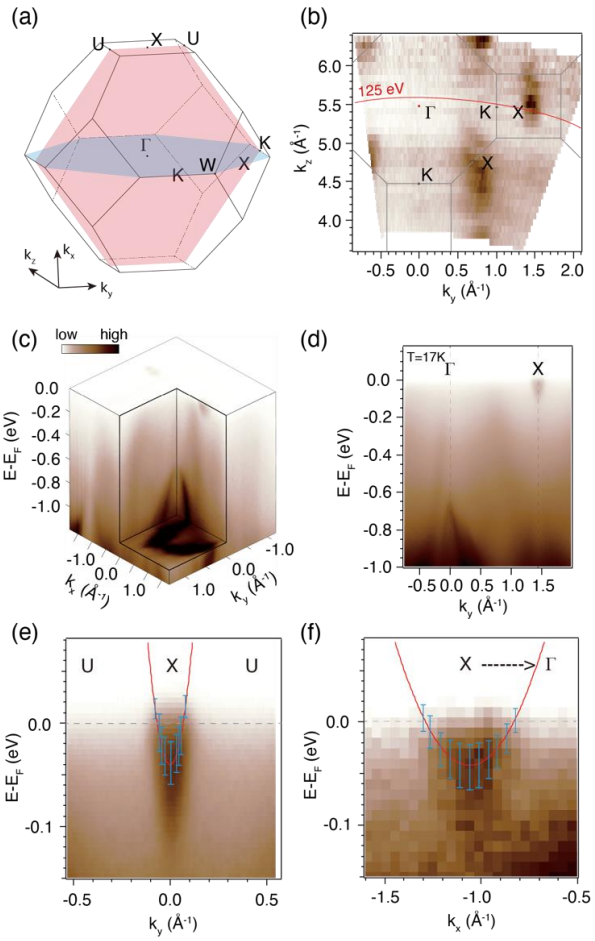

Fig. 3 (a) Brillouin zone with high-symmetry points. In momentum space, the k_x–k_y plane is shown in red, while the k_y–k_z plane is shown in blue. (b) Fermi surface intensity plot in the k_y–k_z plane at k_x = 0. (c) 3D intensity plot of the photoemission data, showing the Fermi surface and electronic structure of ZrNiSn, including two electron pockets at the X point and a hole pocket at the Γ point. (d) ARPES intensity plots along the Γ–X direction, taken as indicated in (c). (e) X–U and (f) X–Γ.

times higher than previous reports involving polycrystalline samples. Furthermore, we studied the effective mass and anisotropic factor of the band, which are important for understanding the origin of high electrical PFs in half-Heusler thermoelectric materials. Our systematic ARPES study on ZrNiSn demonstrated a feasible paradigm for the investigation of the electronic structure of 3D solid materials using ARPES, and provided new insights into the intrinsic electronic structure of half-Heusler systems [7].

Giant Fermi-arc with maximal Chern number in chiral materials

Quasiparticles protected by chiral crystal symmetry have attracted extensive attention because of the large Chern numbers and chiral Fermi arcs on the surface states. In contrast to the fundamental particles in high-energy physics, quasiparticles adhere to crystal symmetry and need not necessarily follow the Poincaré symmetry. According to theoretical predictions, the largest topological charge from multifold fermions has a Chern number of ±4 hosted. However, all ARPES measurements performed to date have confirmed only the existence of chiral Fermi arcs connecting projected multifold fermions. That is, the exact number of Fermi arcs that exist remains unclear.

We conducted ARPES experiments on chiral PtGa crystals using a synchrotron-based ARPES facility, which allowed us to study the surface states, while optimizing both the momentum and energy resolutions. Fermi arcs connecting the time-reversal invariant momenta at the Γ and M points were observed from Fermi surface intensity plots. In addition, measurements of the k_z-dependency

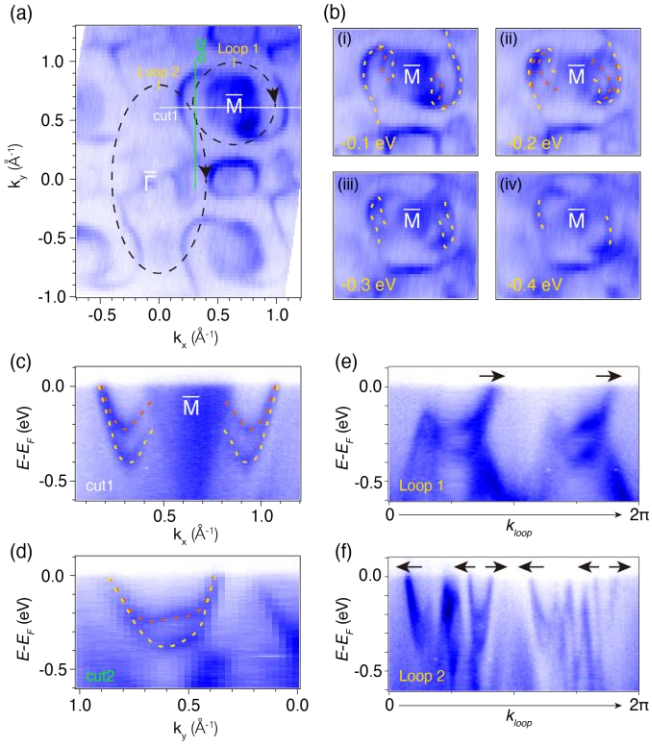

Fig. 4 SOC-induced spin-split Fermi arcs. (a) Fermi surface intensity plots obtained with a photon energy of 60 eV. (b) Series of constant energy maps with different binding energies. The yellow and orange dashed lines are a "by eye" representation of the Fermi arcs. (c, d) ARPES spectra, obtained along the k_x and k_y directions across the Fermi arcs, respectively, as indicated by the white and green lines in (a). (e, f) ARPES spectra along loops 1 and 2, respectively. The paths of the loops are shown in (a), starting from the yellow marks and proceeding clockwise. The black arrows indicate the Fermi velocity of the Fermi-arcs.

confirmed the surface origin of the Fermi arcs. As opposed to bulk bands, which can be calculated with relative precision, the surface state dispersions depend on the atomic termination of real samples. By counting the net number of crossings along the loops surrounding the Γ and M points, we determined the Chern number to be ±4. Our study constituted the first proof of a maximal Chern number in a multifold fermionic system. Moreover, because these Fermi arcs are orders of magnitude larger and highly robust compared with those in other Weyl semimetals, our results provided the basis for further observation and exploration of Fermi-arc-related phenomena in multifold chiral fermions [8].

Projects in progress

Investigation of circular dichroism in chiral materials containing multifold fermions

Recently, the allowed band crossings in condensed matter systems have been considered closely related to elementary particles in high-energy physics. Since the experimental realization of the Dirac semimetal state in Na_3Bi and the Weyl semimetal state in TaAs and WP_2, multifold fermions have been predicted and realized in chiral materials such as CoSi and PtGa. In comparison with Dirac fermions with zero topological charge and Weyl fermions with a Chern number of ±1, multifold fermions in chiral crystals host large Chern numbers and chiral Fermi arcs on their surface states. Unconventional chiral fermions, in particular, hold great promise for experimental applications, as they extend the range of candidate materials available for the observation of topological surface states, bulk chiral transport, and exotic circular photogalvanic effects beyond conventional Weyl semimetals.

However, the winding of electronic wave functions in momentum space, which characterizes the immediate effect of a Berry flux monopole and, by association, the topology of Weyl semimetals, has yet to be elucidated. Nevertheless, recent experimental work on the Weyl semimetal TaAs has shown that orbital-sensitive dichroic effects can be utilized to probe the topological characteristics related to circular dichroism.

Because chiral materials such as PdGa contain multifold fermions, which have non-zero Chern numbers and are separated distinctly in momentum space, they represent an ideal platform for realizing circular dichroism. As such, we plan to perform systematic circular dichroism experiments on chiral materials using ARPES.

References

[1] *Discovery of a three-dimensional topological Dirac semimetal, Na_3Bi, Z. K. Liu, B. Zhou, Y. Zhang, Z. J. Wang, H. M. Weng, D. Prabhakaran, S. K. Mo, Z. X. Shen, Z. Fang, X. Dai, et al., Science **343** (2014) 864.*

[2] *Observation of Weyl nodes in TaAs, B. Q. Lv, N. Xu, H. M. Weng, J. Z. Ma, P. Richard, X. C. Huang, L. X. Zhao, G. F. Chen, C. E. Matt, F. Bisti, et al., Nat. Phys. **11** (2015) 724.*

[3]* *Observation of Weyl nodes in robust Type-II Weyl semimetal WP2, M. -Y. Yao, N. Xu, Q. S. Wu, G. Autès, N. Kumar, V. N. Strocov, N. C. Plumb, M. Radovic, O. V. Yazyev, C. Felser, and J. Mesot, M. Shi, Phys. Rev. Lett. **122** (2019) 176402.*

[4]* *$Mg_3(Bi,Sb)_2$ single crystals towards high thermoelectric performance, Y. Pan, M. Yao, X. Hong, Y. Zhu, F. Fan, L. Imasato, Y. He, C. Hess, J. Fink, J. Yang, et al., Energy Environ. Sci. **13** (2020) 1717.*

[5] *Angle-resolved photoemission spectroscopy and its application to topological materials, B. Lv, T. Qian, and H. Ding, Nat. Rev. Phys. **1** (2019) 609.*

[6]* *Signatures of sixfold degenerate exotic fermions in a superconducting metal $PdSb_2$, N. Kumar, M. Yao, J. Nayak, M. G. Vergniory, J. Bannies, Z. Wang, N. B. M. Schröter, V. N. Strocov, L. Müchler, W. Shi, et al., Adv. Mater. **32** (2020) e1906046, doi.org/10.1002/adma.201906046.*

[7]* *Revealing the intrinsic electronic structure of 3d Half-Heusler Thermoelectric Materials by Angle-Resolved Photoemission Spectroscopy, C. Fu, M. Yao, X. Chen, L. Maulana, X. Li, J. Yang, K. Imasato, F. Zhu, G. Li, G. Auffermann, et al., Adv. Sci.**7** (2020) 1902409, doi.org/10.1002/advs.201902409*

[8]* *Observation of giant spin-split Fermi-arc with maximal Chern number in the chiral topological semimetal PtGa, M. Yao, K. Manna, Q. Yang, A. Fedorov, V. Voroshnin, B. V. Schwarze, J. Hornung, S. Chattopadhyay, Z. Sun, S. N. Guin, et al., Nat. Commun. **11** (2020) 2033.*

[#] Mengyu.Yao@cpfs.mpg.de

[##] Gerhard.Fecher@cpfs.mpg.de